# SPIRAL TRANSITION CURVES AND THEIR APPLICATIONS

Zulfiqar Habib and Manabu Sakai

Received August 21, 2003

Abstract. A method for family of $G^2$ planar cubic Bézier spiral transition from straight line to circle is discussed in this paper. This method is then extended to a pair of spirals between two straight lines or two circles. We derive a family of cubic transition spiral curves joining them. Due to flexibility and wide range of shape control parameters, our method can be easily applied for practical applications like high way designing, blending in CAD, consumer products such as ping-pong paddles, rounding corners, or designing a smooth path that avoids obstacles.

## 1 Introduction

A method for smooth $G^2$ planar cubic Bézier spiral transition from straight line to circle is developed. This method is then extended to a pair of spirals transition between two circles or between two non-parallel straight lines. We also derive an upper bound for shape control parameter and develop a method for drawing a constrained guided planar spiral curve that falls within a closed boundary. The boundary is composed of straight line segments and circular arcs. Our constrained curve can easily be controlled by shape control parameter. Any change in this shape control parameter does not effect the continuity and neighborhood parts of the curve. There are several problems whose solution requires these types of methods. For example:

• Transition curves can be used for blending in the plane, i.e., to round corners, or for smooth transition between circles or straight lines.
• Consumer products such as ping-pong paddles or vase cross section can be designed by blending circles.
• User can easily design rounding shapes like satellite antenna by surface of revolution of our smooth transition curve.
• For applications such as the design of highways or railways it is desirable that transitions be fair. In the discussion about geometric design standards in AASHO (American Association of State Highway officials), Hickerson [7] (p. 17) states that "Sudden changes between curves of widely different radii or between long tangents and sharp curves should be avoided by the use of curves of *gradually increasing or decreasing radii* without at the same time introducing an appearance of forced alignment". The importance of this design feature is highlighted in [2] that links vehicle accidents to inconsistency in highway geometric design.
• A user may wish to design a curve that fits inside a given region as, for example, when one is designing a shape to be cut from a flat sheet of material.
• A user may wish to design a smooth path that avoids obstacles as, for example, when one is designing a robot or auto drive car path.

Parametric cubic curves are popular in CAD applications because they are the lowest degree polynomial curves that allow inflection points (where curvature is zero), so they

2000 *Mathematics Subject Classification.* 65D07, 65D10, 65D17, 65D18.
*Key words and phrases.* $G^2$ continuity; Spiral; Spline; Cubic Bézier; Curvature; *Mathematica*.

are suitable for the composition of $G^2$ blending curves. To be visually pleasing it is desirable that the blend be fair. The Bézier form of a parametric cubic curve is usually used in CAD/CAM and CAGD (Computer Aided Geometric Design) applications because of its geometric and numerical properties. Many authors have advocated their use in different applications like data fitting and font designing. The importance of using fair curves in the design process is well documented in the literature [1, 10].

Cubic curves, although smoother, are not always helpful since they might have unwanted inflection points and singularities (See [3, 9]). Spirals have several advantages of containing neither inflection points, singularities nor curvature extrema (See [5, 4, 13]). Such curves are useful for transition between straight lines and circles. Walton [11] considered a planar $G^2$ cubic transition spiral joining a straight line and a circle. Its use enables us to join two circles forming $C$- and $S$-shaped curves such that all points of contact are $G^2$. Recently, Meek [8] presented a method for drawing a guided $G^1$ continuous planar spline curve that falls within a closed boundary composed of straight line segments and circles. The objectives and shape features of our scheme in this paper are:

- To obtain a family of fair $G^2$ cubic transition spiral curve joining a straight line and a circle.
- To obtain a family of transition curves between two circles or between two non parallel straight lines.
- To simplify and extend the analysis of Walton [11].
- To achieve more degrees of freedom and flexible constraints for easy use in practical applications.
- To find the upper bound for shape control parameter specially for guided $G^2$ continuous spiral spline that falls within a closed boundary composed of straight line segments and circles. Our guided curve has better smoothness than Meek [8] scheme which has $G^1$ continuity.
- Any change in shape parameter does not effect continuity and neighborhood parts of our guided spline. So, our scheme is completely local.

The organization of our paper is as follows. Next section gives a brief discussion of the notation and conventions for the cubic Bézier spiral with some theoretical background and description of method. Its use for the various transitions encountered in general curve, guided curve and practical applications is analysed followed by illustrative examples, concluding remarks and future research work.

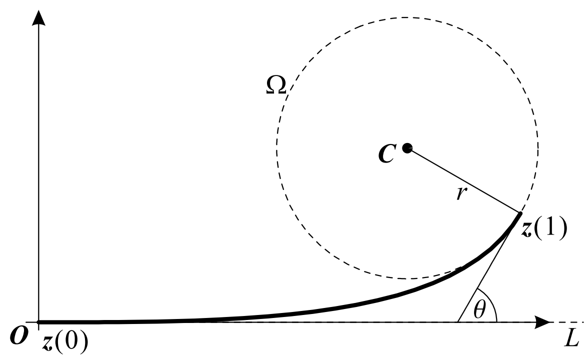


Figure 1: Straight line to circle transition.

**2 Background and Description of Method** Let $L$ be a straight line through origin $\boldsymbol{O}$ and a circle $\Omega$ of radius $r$ centered at $\boldsymbol{C}$ (see Fig. 1). We consider a cubic transition $\boldsymbol{z}(t)(=(x(t),y(t))), 0 \le t \le 1$ of the form

$$(1)\qquad \begin{aligned} x'(t)(=u(t)) &= u_0(1-t)^2 + 2u_1 t(1-t) + u_2 t^2 \\ y'(t)(=v(t)) &= v_0(1-t)^2 + 2v_1 t(1-t) + v_2 t^2 \end{aligned}$$

Its signed curvature $\kappa(t)$ is given by

$$(2)\qquad \kappa(t)\left(=\frac{\boldsymbol{z}'(t)\times\boldsymbol{z}''(t)}{\|\boldsymbol{z}'(t)\|^3}\right)=\frac{u(t)v'(t)-u'(t)v(t)}{\{u(t)^2+v^2(t)\}^{3/2}}$$

where $\times$ stands for the two-dimensional cross product $(x_0,y_0)\times(x_1,y_1)=x_0y_1-x_1y_0$ and $\|\bullet\|$ means the Euclidean norm. For later use, consider

$$(3)\qquad \begin{aligned} &\left\{u^2(t)+v^2(t)\right\}^{5/2}\kappa'(t)=\{u(t)v''(t)-u''(t)v(t)\}\left\{u^2(t)+v^2(t)\right\} \\ &-3\{u(t)v'(t)-u'(t)v(t)\}\{u(t)u'(t)+v(t)v'(t)\}\,(=w(t)) \end{aligned}$$

Then, we require for $0<\theta<\pi/2$

$$(4)\qquad \boldsymbol{z}(0)=(0,0),\quad \boldsymbol{z}'(0)\parallel(1,0),\quad \kappa(0)=0,\quad \boldsymbol{z}'(1)\parallel(\cos\theta,\sin\theta),\quad \kappa(1)=1/r$$

Then, the above conditions require

**Lemma 1** *With a positive parameter* $d$

$$(5)\qquad u_1=\frac{d^2}{2r\sin\theta},\quad u_2=d\cos\theta,\quad v_0=0,\quad v_1=0,\quad v_2=d\sin\theta$$

*where* $\boldsymbol{z}'(0)=(u_0,0)$ *and* $\boldsymbol{z}'(1)=d(\cos\theta,\sin\theta)$.

We introduce a pair of parameters $(m,q)$ for $(u_0,d)$ as

$$(6)\qquad u_0=mu_1, d=qr$$

Then,

$$(7)\qquad u_0=\frac{mrq^2}{2\sin\theta},\quad u_1=\frac{rq^2}{2\sin\theta},\quad u_2=qr\cos\theta,\quad v_0=v_1=0,\quad v_2=qr\sin\theta$$

from which

$$(8)\qquad \begin{aligned} x(t)&=\frac{qrt}{6\sin\theta}\left[q\left\{(3-2t)t+m(3-3t+t^2)\right\}+t^2\sin 2\theta\right] \\ y(t)&=\frac{qrt^3\sin\theta}{3} \end{aligned}$$

Walton ([11]) considered a cubic curve $\boldsymbol{z}(t)(=(x(t),y(t)), 0\le t\le 1$ of the form

$$(9)\qquad \boldsymbol{z}(t)=\boldsymbol{b}_0(1-t)^3+3\boldsymbol{b}_1 t(1-t)^2+\boldsymbol{b}_2(1-t)t^2+\boldsymbol{b}_3 t^3$$

where Bézier points $\boldsymbol{b}_i, 0 \le i \le 3$ are defined as follows

$$\boldsymbol{b}_1 - \boldsymbol{b}_0 = \boldsymbol{b}_2 - \boldsymbol{b}_1 = \frac{25r\tan\theta}{54\cos\theta}(1,0), \quad \boldsymbol{b}_3 - \boldsymbol{b}_2 = \frac{5r\tan\theta}{9}(\cos\theta, \sin\theta) \tag{10}$$

Simple calculation gives

$$\begin{aligned} x'(t)(= u(t)) &= u_0(1-t)^2 + 2u_1 t(1-t) + u_2 t^2 \\ y'(t)(= v(t)) &= v_0(1-t)^2 + 2v_1 t(1-t) + v_2 t^2 \end{aligned} \tag{11}$$

where

$$u_0 = u_1 = \frac{25r\tan\theta}{18\cos\theta}, \quad u_2 = \frac{5r\sin\theta}{3}, \quad v_0 = v_1 = 0, \quad v_2 = \frac{5r\tan\theta\sin\theta}{3} \tag{12}$$

Hence, note that their method is our special case with $m = 1$ and $q = 5\tan\theta/3$.

With help of a symbolic manipulator, we obtain

$$\kappa'\left(\frac{1}{1+s}\right) = \frac{8(1+s)^5\left(\sum_{i=0}^{5} a_i s^i\right)\sin^3\theta}{r\left\{q^2s^2(2+ms)^2 + 2qs(2+ms)\sin 2\theta + 4\sin^2\theta\right\}^{5/2}} \tag{13}$$

where

$$\begin{aligned} &a_0 = 4\{3q\cos\theta - (4+m)\sin\theta\}\sin\theta, a_1 = 2\left\{6q^2 - q(5-4m)\sin 2\theta - 10m\sin^2\theta\right\} \\ &a_2 = 2q\{(-2+13m)q - 2m(4-m)\sin 2\theta\}, a_3 = 2mq\{(-3+10m)q - 2m\sin 2\theta\} \\ &a_4 = 5m^3q^2, a_5 = m^3q^2 \end{aligned}$$

Hence, we have a sufficient spiral condition for a transition curve $\boldsymbol{z}(t), 0 \le t \le 1$, i.e., $a_i \ge 0, 0 \le i \le 5$:

**Lemma 2** *The cubic segment $\boldsymbol{z}(t), 0 \le t \le 1$ of the form (1) is a spiral satisfying (5) if $m > 3/10$ and*

$$\begin{aligned} &q \ge q(m,\theta)\Bigg(= Max\left[\frac{(4+m)\tan\theta}{3}, \ \frac{2m(4-m)\sin 2\theta}{13m-2}, \ \frac{2m\sin 2\theta}{10m-3},\right. \\ &\left.\frac{1}{6}\left\{(5-4m)\cos\theta + \sqrt{60m + (5-4m)^2\cos^2\theta}\right\}\sin\theta\right]\Bigg) \end{aligned} \tag{14}$$

As in [11], we can require an additional condition $\kappa'(1) = 0$. Then $a_0 = 0$, i.e., $q = \frac{4+m}{3}\tan\theta$. Therefore the above condition (14) gives a spiral one:

**Lemma 3** *The cubic segment $\boldsymbol{z}(t), 0 \le t \le 1$ of the form (1) is a spiral satisfying (5) and $\kappa'(1) = 0$ for $\theta \in (0, \pi/2]$ if $m \ge 2(-1+\sqrt{6})/5(= c_0)(\approx 0.5797)$*

Proof. Letting $z = \tan\theta(> 0)$, we only have to notice that the terms in brackets of (13) reduce

$$\begin{aligned} &\frac{(4+m)z}{3}(= A_1), \frac{4m(4-m)z}{(13m-2)(1+z^2)}(= A_2), \frac{4mz}{(10m-3)(1+z^2)}(= A_3), \\ &\frac{z\left\{5 - 4m + \sqrt{25 + 16m^2 + 20m(1+3z^2)}\right\}}{6(1+z^2)}(= A_4) \end{aligned}$$

Here, we have to check that the first quantity is not less than the remaining three ones where

$$A_1 \geq A_2 \quad (m \geq \frac{1}{25}(-1+\sqrt{201})(\approx 0.5270))$$
$$A_1 \geq A_3 \quad (m \geq \frac{1}{20}(-25+\sqrt{1105})(\approx 0.4120))$$
$$A_1 \geq A_4 \quad (m \geq c_0)$$

**2.1 Circle to Circle Spiral Transition** A method for straight line to circle transition is being extended to $C$- or $S$-shaped transition between two circles $\Omega_0$, $\Omega_1$ with centers $\mathrm{C}_0$, $\mathrm{C}_1$ and radii $r_0$, $r_1$ respectively. Now, $\boldsymbol{z}(t,r)(=(x(t,r),y(t,r)), 0 \leq t \leq 1$ denotes the cubic spline satisfying (5). Then, a $C$-shaped pair of cubic curves: $(x(t,r_0),y(t,r_0))$ and $(-x(t,r_1),y(t,r_1))$ is considered to be a pair of spiral transition curves joining two circles with radii $r_0, r_1$, respectively. Then, the distance $\rho(=\|\mathrm{C}_0-\mathrm{C}_1\|)$ of the centers of the two circles is given with $q \geq q(m,\theta)$

$$\rho = \sqrt{g_1^2(r_0+r_1)^2 + g_2^2(r_0-r_1)^2} \tag{15}$$

where

$$g_1(=g_1(m,\theta,q)) = \left(\frac{1}{6\sin\theta}\right)\left\{(1+m)q^2 + q\sin 2\theta - 6\sin^2\theta\right\}$$
$$g_2(=g_2(m,\theta,q)) = \frac{1}{3}\left(q\sin\theta + 3\cos\theta\right) \tag{16}$$

A simple calculation gives

$$(17)\quad \begin{aligned} &(i) \quad (g_1(m,\theta,q(m,\theta)), g_2(m,\theta,q(m,\theta))) \to (0,1) \quad (\theta \to 0) \\ &(ii) \quad g_1(m,\theta,q(m,\theta)), g_2(m,\theta,q(m,\theta)) \to \infty \quad (\theta \to \frac{\pi}{2}) \end{aligned}$$

Hence we have

**Theorem 1** *If $\|C_0 - C_1\| > |r_0 - r_1|$, a $C$-shaped pair of cubic curves $(x(t,r_0),y(t,r_0))$ and $(-x(t,r_1),y(t,r_1))$ is a pair of spiral transitions of $G^2$-continuity from $\Omega_0$ to $\Omega_1$ for a selection of $\theta \in (0,\pi/2)$.*

Next, a pair of an $S$-shaped cubic curves $(x(t,r_0),y(t,r_0))$ and $(-x(t,r_1),-y(t,r_1))$ is considered to be a pair of spiral transition curves from $\Omega_0$ to $\Omega_1$. Then, the distance $\rho(=\|\mathrm{C}_0-\mathrm{C}_1\|)$ of the centers of the two circles is given by

$$\rho = \sqrt{g_1^2 + g_2^2}(r_0+r_1) \tag{18}$$

Note (16) to obtain

**Theorem 2** *If $\|C_0 - C_1\| > r_0 + r_1$, an $S$-shaped pair of cubic curves $(x(t,r_0),y(t,r_0))$ and $(-x(t,r_1),-y(t,r_1))$ is a pair of spiral transitions of $G^2$-continuity from $\Omega_0$ to $\Omega_1$ for a selection of $\theta \in (0,\pi/2)$.*

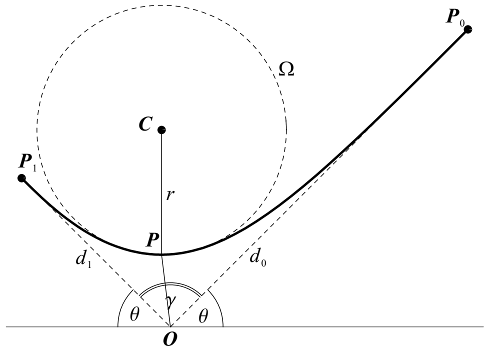


Figure 2: Transition between two straight lines.

**2.2 Straight Line to Straight Line Spiral Transition** Here, we have extended the idea of straight line to circle transition and derived a method for Bézier spiral transition between two nonparallel straight lines (see Fig. 2). We note the following result that is of use for joining two lines. For $0 < \theta < \pi/2$, we consider a cubic curve satisfying

(19) $$\boldsymbol{z}(0) = (0,0), \quad \boldsymbol{z}'(0) \parallel (1,0), \quad \kappa(0) = 1/r, \quad \boldsymbol{z}'(1) \parallel (\cos\theta, \sin\theta), \quad \kappa(1) = 0$$

Since Bézier curves are affine invariant, a cubic Bézier spiral can be used in a coordinate free manner. Therefore transformation, i.e., rotation, translation, reflection with respect to $y$-axis and change of variable $t$ with $1-t$ to (9) gives $\boldsymbol{z}(t)(=(x(t), y(t))$ by

(20) $$x(t) = \frac{qrt}{6\sin\theta}\left[qt\{3-(2-m)t\}\cos\theta + 2(3-3t+t^2)\sin\theta\right]$$
$$y(t) = \frac{q^2rt^2}{6}\{3-(2-m)t\}$$

Now, $\boldsymbol{z}(t,m,\theta)(=(x(t,m,\theta), y(t,m,\theta)), 0 \le t \le 1$ denotes the cubic spline satisfying (19). Assume that the angle between two lines is $\gamma$ $(< \pi)$. Then, $(x(t,m,\theta_0), y(t,m,\theta_0))$ of the form (21) with $q = q_0(\ge q(m,\theta_0))$ and $(-x(t,n,\theta_1), y(t,n,\theta_1))$ of the form (21) with $q_1(\ge q(n,\theta_1))$ with $\theta_0 + \theta_1 = \pi - \gamma$ is a pair of spiral transition curves whose join is $G^3$. In addition, when $\theta_0 = \theta_1 (= \theta = (\pi-\gamma)/2)$ are fixed and $m, n \ge c_0$ (then, note $q_0 = (4+m)/3\tan\theta$ and $q_1 = (4+n)/3\tan\theta$), the distances between the intersection $\boldsymbol{O}$ of the two lines and the the end points $\boldsymbol{P}_i, i = 0,1$ of the transition curves are given by $d(m,n,r,\theta)$ and $d(n,m,r,\theta)$ where

(21) $$d(m,n,r,\theta) = (r/c)\left\{4+(3+m)^3+3(3+n)\right\}, \quad c = 54\cos^2\theta/\sin\theta$$

Here we derive a condition on $r$ for which the following system of equations has the solutions $m, n (\ge c_0)$ for given nonnegative $d_0, d_1$:

(22) $$d(m,n,r,\theta) = d_0, \quad d(n,m,r,\theta) = d_1$$

Let $(\alpha, \beta) = (3+m, 3+n)$ reduce the above system to

(23) $$\alpha^3 + 3\beta = \lambda(= cd_0/r - 4), \quad \beta^3 + 3\alpha = \mu(= cd_1/r - 4)$$

where require $m, n \ge c_0$ to note $\alpha, \beta \ge c_1 (= c_0 + 3)$ and $\lambda, \mu \ge c_2 (= c_1^3 + 3c_1)$. Delete $\alpha$ from (1.23) to get a quartic equation $f(\beta) = 0$:

(24) $$f(\beta) = \beta^9 - 3\mu\beta^6 + 3\mu^2\beta^3 - 81\beta + 27\lambda - \mu^3$$

Restrictions: $\alpha, \beta \geq c_1$ require that at least one root $\beta$ of $f(\beta) = 0$ must satisfy

$$c_1 \leq \beta \leq (\mu - 3c_1)^{1/3} \tag{25}$$

Intermediate value of theorem gives a sufficient condition: $f(c_1) \leq 0$ and $f((\mu - 3c_1)^{1/3}) \geq 0$ where

$$\begin{aligned} f(c_1) &= -\mu^3 + 3c_1^3\mu^2 - 3c_1^6\mu + 27\lambda + c_1^9 - 81c_1 = -\left\{\mu - c_1^3 - 3(\lambda - 3c_1)^{1/3}\right\} \times \\ &\left[(\mu - c_2)^2 + 3\left\{2c_1 + (\lambda - 3c_1)^{1/3}\right\}(\mu - c_2) + 9\left\{c_1^2 + c_1(\lambda - 3c_1)^{1/3} + (\lambda - 3c_1)^{2/3}\right\}\right] \\ f((\mu - 3c_1)^{1/3}) &= 27\left\{\lambda - c_1^3 - 3(\mu - 3c_1)^{1/3}\right\} \end{aligned} \tag{26}$$

Since the quantity in brackets is positive for $\mu \geq c_2$, the sufficient one reduces to

$$\lambda - c_1^3 \geq 3(\mu - 3c_1)^{1/3}, \quad \mu - c_1^3 \geq 3(\lambda - 3c_1)^{1/3} \tag{27}$$

Note $\lambda, \mu \geq c_2$ to obtain

**Lemma 4** *Given $d_0, d_1$, assume that $r$ satisfies $\lambda - c_1^3 \geq 3(\mu - 3c_1)^{1/3} \geq 0, \mu - c_1^3 \geq 3(\lambda - 3c_1)^{1/3} \geq 0$. Then the system of (23) has the required solutions $\alpha, \beta$ $(\geq c_1)$.*

Note $\lambda, \mu = O(1/r), r \to 0$ to obtain that a small value of $r$ makes the inequalities (27) be valid for any $d_0, d_1$. Next, for an upper bound for $r$, we require

**Lemma 5** *If $d_0 \geq d_1$, then $\mu - c_1^3 = 3(\lambda - 3c_1)^{1/3}$ and $\lambda, \mu \geq c_2$ by (23) has a unique positive solution $r^*$.*

Proof. Let $t = 1/r$ to reduce $\mu - c_1^3 = 3(\lambda - 3c_1)^{1/3}$ to

$$f(t) \left(= (cd_1t - 4 - c_1^3)^3 - 27(cd_0t - 4 - 3c_1)\right) = 0 \tag{28}$$

where $\lambda, \mu \geq c_2$ are equivalent to $t \geq (c_2 + 4)/(cd_1)$. First, note with $d_0 = k^2 d_1$ $(k \geq 1)$

$$f(+\infty) = +\infty, \quad f\left(\frac{c_2 + 4}{cd_1}\right) = -27(c_1 + 1)(c_1^2 - c_1 + 4)(k^2 - 1)(\leq 0)$$

In addition, $f(t)$ has its relative maximum at $t = (c_1^3 + 4 - 3k)/(cd_1)\,(< (c_2 + 4)/(cd_1))$. Therefore, $f(t) = 0$ has just one root $t = t^*(= 1/r^*)\,(\geq (c_2 + 4)/(cd_1))$. As $r$ increases from zero, 'equality" in the second inequality of (27) is first valid. Hence, we obtain

**Theorem 3** *Assume that $d_0 \geq d_1$. Then the system of equation (22) in $m, n$ $(\geq c_0)$ is solvable for $0 < r \leq r^*$ where $r^*$ is the positive root no greater than $cd_1/(c_2 + 4)$:*

$$\left\{(4 + c_1^3)r - cd_1\right\}^3 - 27r^2\left\{(4 + 3c_1)r - cd_0\right\} = 0, \quad c_1 = c_0^3 + 3c_0 \tag{29}$$

*Then, for the angle $\gamma$ $(< \pi)$ between the two straight lines with $\theta = (\pi - \gamma)/2$, $(x(t, m, \theta),$ $y(t, m, \theta))$, $q = \{(4 + m)/3\}\tan\theta$ of the form (21) and $(-x(t, n, \theta), y(t, n, \theta))$, $q = \{(4 + n)/3\}\tan\theta$ of the form (21) is a pair of spiral transition curves between the two lines.*

This result enables the pair of the spirals to pass through the given points of contact on the non-parallel two straight lines. For example, Lemma 4 shows that for $\gamma = \pi/3$ and $(d_0, d_1) = (3, 1)$ (Figure 8 in Numerical Example), $r^* \approx 0.2326$. For fixed $\theta$, $r^*$ could be enlarged as follows. That is, for $\theta = \pi/3$, we only have to notice $q(m, \theta) = \{(4 + m)/3\}\tan\theta$

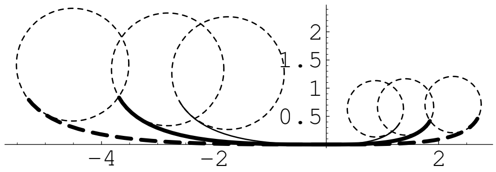


Figure 3: Graphs of $\boldsymbol{z}(t)$ with $(r_0, r_1, \theta) = (0.5, 1, \pi/3)$.

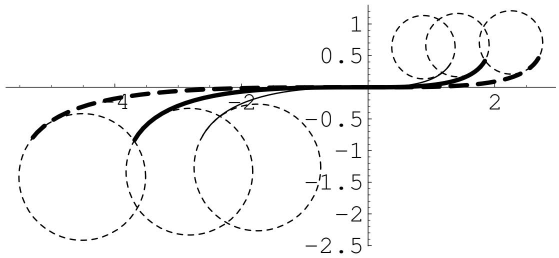


Figure 4: Graphs of $\boldsymbol{z}(t)$ with $(r_0, r_1, \theta) = (0.5, 1, \pi/3)$.

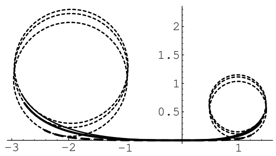


Figure 5: Graphs of $\boldsymbol{z}(t)$ with $(r_0, r_1) = (0.5, 1)$ and $\|\mathrm{C}_0 - \mathrm{C}_1\| = 3$.

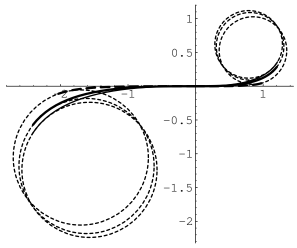


Figure 6: Graphs of $\boldsymbol{z}(t)$ with $(r_0, r_1) = (0.5, 1)$ and $\|\mathrm{C}_0 - \mathrm{C}_1\| = 3$.

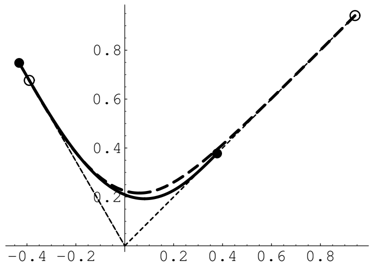


Figure 7: Graphs of $\boldsymbol{z}(t)$ with $(r, \alpha, \theta_0, \theta_1) = (0.2, 5\pi/12, \pi/4, \pi/3)$.

for $m \geq \bar{c}_0 = (\sqrt{409} - 17)/10(\approx 0.3223)$ instead of $m \geq c_0(\approx 0.5797)$. Then, for $(d_0, d_1) = (3, 1)$, $r^* \approx 0.2742$ with $(m, n) \approx (2.38, 0.32)$.

Finally we remark the next result for the limiting case $(r \to 0)$:

$$\boldsymbol{P} = \frac{r}{18}\left((m-n)\tan\theta, -(8+m+n)\tan^2\theta\right) \to \boldsymbol{O}(= (0,0)) \tag{30}$$

since $r \to 0$ gives $m, n = O\left(r^{-1/3}\right)$ from (21)-(22). Hence, the pair of spirals tends to the segments $\boldsymbol{P}_0\boldsymbol{O}$ and $\boldsymbol{O}\boldsymbol{P}_1$ as $r \to 0$. To keep the transition curve within a closed boundary, value of shape control parameter $r$ can be derived from (21) when control points and boundary information are given. A constrained guided curve is shown in Figure 10.

**3 Numerical Examples** This section gives numerical examples for $q = q(m, \theta)$ to assure our theoretical analysis. Figures 3-4 give family of transition curves between two circles with $m = 1.5$ (dotted), 1 (bold) and 0.6 (normal). Figures 5-6 give family of transition curves with fixed distance between two circles for $(m_0, m_1)$ =(3, 3) (dotted), (1, 1) (bold), (0.6, 0.6) (normal). Figure 7 shows the graphs of the family of transition curves between two straight lines for $(m_0, m_1) = (3, 0.8)$ (dotted) and (1, 1) (bold). In Figure 8, the distances between the intersection of the two curves and the points of contact are 3 and 1 with $r = 0.1$ (dotted) and 0.2 (bold). By (22), for $r = 0.1$, $(m_0, m_1) \approx (4.65, 2.05)$ and for $r = 0.2$, $(m_0, m_1) \approx (3.02, 0.82)$. Figure 9 illustrates a vase cross-section incorporating one $C$ transition and two $S$ transitions. Ends of curves are shown with small circles. In Figure 10, a constrained $G^2$ continuous spiral spline uses straight line to straight line transition and straight line to circle transition. The boundary is composed of straight line segments and circular arcs. This figure also shows that all segments have completely local control. The data for boundary and control points has been taken from Figure 8 in [8]. Figure 11 is a satellite antenna obtained by surface of revolution of $G^2$ cubic Bézier spiral. Figure 12 is vase profile using $G^2$ cubic Bézier spiral segments. It uses straight line segments and line to line spiral segments. Control points are calculated from rational cubic spline [6] with unit parametrization for figure 12(a) and chord-length parametrization for figure 12(b). Finally, curves in figure 12 are used for surface of revolution shown in figure 13.

**4 Conclusion and Future Research Work** The cubic Bézier spiral is a reasonable alternative to the clothoid for practical applications such as highway and railway design. We introduced a family of $G^2$ spiral transition curves between two circles and straight lines. Further, we presented a very simple and flexible scheme offering more degree of freedom. To guarantee the absence of interior curvature extremum (i.e., spiral segment) in transition curve, user can select any value of parameter $m$ greater than 0.5797. On the other hand it must be 1 in Walton [11] scheme. Similarly, straight line to straight line transition has wide selection of shape control parameters and their values as demonstrated in Figures 3-10. We provided four degrees of freedom for the curve designer to use as shape control parameters by choosing their values. Walton offered only one degree of freedom in [11]. We also presented constrained guided $G^2$ continuous spiral spline within a closed boundary. Our guided curve scheme is more smoother and offer better local control than recent research work of Meek in [8] which has $G^1$ continuity. So our scheme is not only very simple but also reasonable and comfortable for lot of different kind of practical applications.

A PH (Pythagorean Hodograph) quintic curve has the attractive properties that its arc-length is a polynomial of its parameter, and its offset is rational. A quintic is the lowest degree PH curve that may have an inflection point. These curves have been discussed in [12]. In our future research work, the results for the cubic $G^2$ spiral curve will be extended

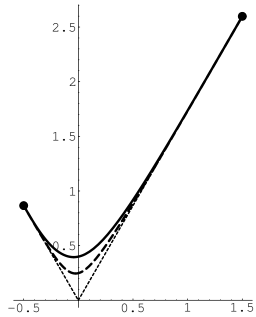


Figure 8: Graphs of $\boldsymbol{z}(t)$ with $\gamma = \theta_0 = \theta_1 = \pi/3$.

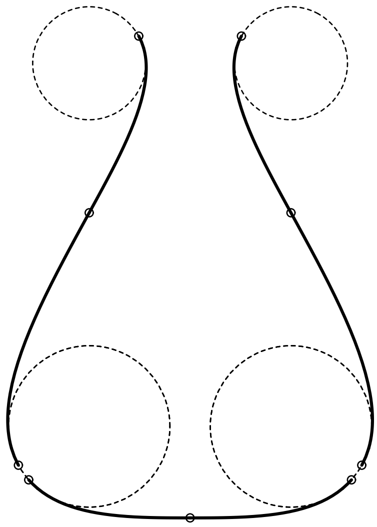

Figure 9: Vase cross-section.

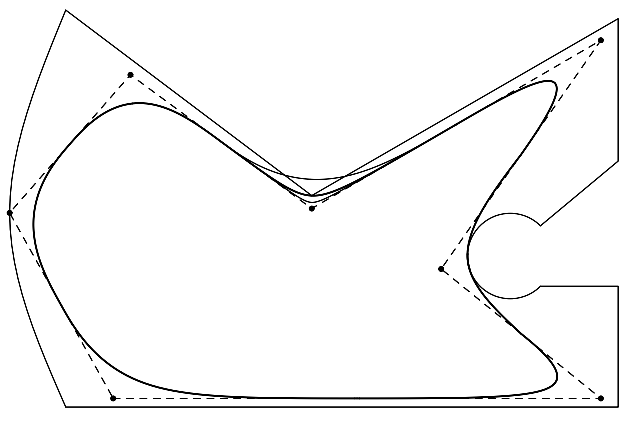

Figure 10: A curve constrained by a closed boundary.

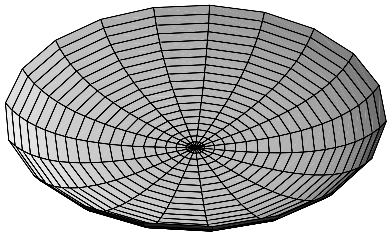

Figure 11: Satellite antenna.

(a) Unit parametrization

(b) Chord-length parametrization

Figure 12: Vase profile with $G^2$ cubic Bézier spiral segments.

(a) Unit parametrization

(b) Chord-length parametrization

Figure 13: Shaded rendition of segments in Figure 12.

to family of PH quintic $G^2$ spiral transition curves. We will try for simplified and more flexible shape parameter values.

**Acknowledgement**

We acknowledge the financial support of JSPS (Japan Society for the Promotion of Science).

## References

[1] G. Farin. *NURB Curves and Surfaces.* A K Peters, 1995.

[2] G. M. Gibreel, S. M. Easa, Y. Hassan, and I. A. El-Dimeery. State of the art of highway geometric design consistency. *ASCE Journal of Transportation Engineering*, 125(4):305–313, 1999.

[3] Z. Habib and M. Sakai. $G^2$ two-point Hermite rational cubic interpolation. *International Journal of Computer Mathematics*, 79(11):1225–1231, 2002.

[4] Z. Habib and M. Sakai. $G^2$ planar cubic transition between two circles. *International Journal of Computer Mathematics*, 80(8):959–967, 2003.

[5] Z. Habib and M. Sakai. Quadratic and T-cubic spline approximations to a planar spiral. *Scientiae Mathematicae Japonicae*, 57(1):149–156, 2003. :e7, 107-114, http://www.jams.or.jp/scmjol/7.html.

[6] Z. Habib and M. Sarfraz. A rational cubic spline for the visualization of convex data. pages 744–748, USA, July 2001. The Proceedings of IEEE International Conference on Information Visualization-IV'01-UK, IEEE Computer Society Press.

[7] T. F. Hickerson. *Route Location and Design.* McGraw-Hill, New York, 1964.

[8] D. S. Meek, B. Ong, and D. J. Walton. A constrained guided $G^1$ continuous spline curve. *Computer Aided Design*, 35:591–599, 2003.

[9] M. Sakai. Osculatory interpolation. *Computer Aided Geometric Design*, 18:739–750, 2001.

[10] B. Su and D. Liu. *Computaional Geometry: Curve and Surface Modeling.* Academic Press, New York, 1989.

[11] D. J. Walton and D. S. Meek. A planar cubic Bézier spiral. *Computational and Applied Mathematics*, 72:85–100, 1996.

[12] D. J. Walton and D. S. Meek. A Pythagorean hodograph quintic spiral. *Computer Aided Design*, 28:943–950, 1996.

[13] D. J. Walton and D. S. Meek. Curvature extrema of planar parametric polynomial cubic curves. *Computational and Applied Mathematics*, 134:69–83, 2001.

Department of Mathematics and Computer Science, Graduate School of Science and Engineering, Kagoshima University, Kagoshima 890-0065, Japan.
Phone: ++81-99-2858049; Fax: ++81-99-2858051
*Email: habib@eniac.sci.kagoshima-u.ac.jp; msakai@sci.kagoshima-u.ac.jp*